CrossMark

Simultaneous wireless energy transfer and spectrum sharing with primary data relaying in cognitive radio networks

Zhiyuan Yu[1,2], Chao Zhai[1] and Ju Liu[1,2*]

Abstract

Spectrum sharing and energy harvesting (EH) are promising techniques to enhance the spectrum and energy efficiency of wireless networks. In this paper, we propose a spectrum sharing scheme based on the cooperative energy and data transfer in both the time and space domains. When the primary base station (PB) transfers energy to the primary user (PU), the secondary user (SU) can transmit its own data simultaneously, and the interference of secondary data transmission becomes beneficial to improve the EH efficiency of the PU. Furthermore, the SU can assist the primary data relaying using the Alamouti coding technique to improve the link robustness through introducing the space diversity. With the energy and data cooperation from the SU, the primary data can be more quickly and reliably delivered, and hence more opportunities can be achieved for the spectrum sharing. Considering the dependence of the energy and data transfer, the throughput of both systems is investigated. The time allocation between EH and data transmission can be numerically determined by maximizing the throughput of secondary system under the throughput constraint of primary system. Performance results are presented to validate our theoretical analysis and provide some guidelines for the network configuration.

Keywords: Spectrum sharing, Wireless energy transfer, Cooperative relaying, Alamouti coding, Cognitive radio

1 Introduction

The radio frequency (RF) energy harvesting (EH) is a promising technique that enables the smart power-limited devices to harvest energy from the electromagnetic radiation [1]. Researchers have shown that the maximal harvested energy is about 7.0 and 1.0 μW at the free space distance of 40 m over 2.4 and 900 MHz, respectively [2]. In this way, the harmful interference becomes a source of energy, which can improve the energy efficiency and thus significantly prolong the network lifetime [3, 4]. The rapid advancement of the EH materials and devices makes the network coupling with EH devices a reality [5], e.g., the Powerharvester Receivers designed by the Powercast can harvest the RF energy to charge the remote battery-free devices [6]. A highly-efficient rectenna was designed in [7] to improve the output power of the direct current as well

as the power sensitivity, which can be used for the EH in the wireless sensor network.

1.1 Related work

Spectrum sharing has been intensively studied to deal with the increasing requirements of wireless data transmissions over the limited but under-utilized bandwidth. In this context, the unlicensed users also known as the secondary users (SUs) are allowed to access the licensed spectrum of the high-priority primary users (PUs), but under the constraint that the transmission requirements of PUs should be strictly protected.

To improve the spectrum efficiency, many spectrum sharing schemes have been proposed [8–12]. In the space domain, the SU can use a fraction of its power to relay the primary data, while the remaining power is used for its own data transmission [8]. Huang et al. studied the capacity tradeoff between cellular and mobile ad hoc networks for the underlay and overlay spectrum sharing schemes [9]. In the multiuser scenario, a SU can be selected to

*Correspondence: juliu@sdu.edu.cn
[1]School of Information Science and Engineering, Shandong University, 27 Shanda Nanlu, 250100 Jinan, China
[2]National Mobile Communications Research Laboratory, Southeast University, 2 Sipailou, 210096 Nanjing, China

Springer Open

Yu *et al. EURASIP Journal on Wireless Communications and Networking* (2017) 2017:9

Page 2 of 13

assist the primary data transmission to tolerate the interference caused by the secondary data transmission from another selected SU [10]. In the frequency domain, the SU can help relay the primary data to exchange for some disjoint bandwidth for its own data transmission [11]. To combat the low efficiency of half-duplex cooperative protocols, Zhai et al. proposed the spectrum sharing based on the two-path successive relaying [12], where two SUs can alternatively and successively relay the primary data and transmit their own data using the superposition coding technique, while the successive interference cancelation (SIC) techniques is adopted by the receivers to decode the desired information.

The RF signal can carry not only information but also energy, so there exists an energy-rate tradeoff for the simultaneous wireless information and power transfer (SWIPT) [13, 14]. Huang et al. deployed the orthogonal frequency division multiplexing (OFDM) and transmit beamforming for the SWIPT in a broadband system [15]. For the large-scale network, Krikidis studied the cooperative relay protocol to show the tradeoff between the outage performance and the wireless energy transfer (WET) [3]. For the stochastic networks, the cooperative energy transfer and data relaying protocol was proposed by properly modeling the locations of users as Poisson point process [16]. Rubio et al. analyzed the tradeoff between the sum-rate and the energy constraints in the multiuser multiple-input multiple-output (MIMO) system [17]. The harvest-then-transmit protocol was proposed in [18], where the terminals should first harvest the ambient RF energy, and then transmit data using the harvested energy. Reference [19] implemented the power beacons in the cellular network to transfer the microwave power to the mobile devices to support their uplink data transmissions to the base stations.

The EH-based spectrum sharing has drawn intensive research interests nowadays. The optimal mode selection policy was designed by balancing the trade-off between spectrum accessing and energy harvesting [20]. The SUs can opportunistically harvest the RF energy from the nearby PUs and reuse the spectrum to send their signals if they lie outside the exclusive regions of all the PUs [21]. Mousavifar et al. proposed the spectrum sharing scheme that the source and the relay can harvest energy from the PUs and the information of source is forwarded to the destination by the relay [22]. The joint information and energy cooperation between primary and secondary systems is investigated in [23], where the SUs can help the primary data transmissions to acquire the energy and spectrum for the secondary data transmission. The SUs can be scheduled to access the selected channel for the data transmission or harvest energy by designing a learning algorithm [24]. Park et al. derived the upper bound of the achievable throughput

for the EH SUs under the energy causality and collision constraints [25].

Although there exist some related works about the EH-based spectrum sharing for different network structures, it is still necessary to further improve the spectral and energy efficiency. Our proposed transmission strategy is different from those of above papers. In our paper, the single-antenna UE and SU can form the virtual antenna array in the cooperative period and the spatial diversity can be achieved by using Alamouti coding to enhance the reliability of data transmission. As a result, the energy and spectral efficiency of the cognitive radio network can be greatly improved.

1.2 Motivation and contribution

In the cognitive radio network, the time-switching or the power-splitting techniques can be adopted by the PU for the EH and information decoding [13]. Usually, the valuable spectrum is either used solely for the energy transfer or for the data transmission. It is necessary to design flexible schemes to efficiently utilize the spectrum to realize both the EH and the spectrum sharing. Furthermore, the SU can use its energy to relay the primary data to improve the link robustness and hence strive for more opportunities for the spectrum sharing. It is a win-win game for both systems by considering the resource complementary that the PUs own spectrum but lack energy, while the SUs have enough energy but lack spectrum.

We propose a spectrum sharing scheme based on the cooperative energy and data transfer for the cognitive radio network, where a secondary link is overlaid with a primary link. Each terminal is assumed to be equipped with one omnidirectional antenna and the similar assumption is made in [18, 26]. In the primary system, the user equipment (UE) has the capability of harvesting energy from the RF signals. All the other terminals are assumed to have the stable power supply. Compared with the standalone primary system, with the energy assistance from the secondary link, the UE will get more energy and be charged quickly. Also, the primary data from the UE can be delivered more reliably. The main contributions of this work are summarized as:

- In the EH period of our proposed scheme, the SU can transmit its own data using the licensed spectrum, of which the interference can help recharge the UE. When the UE transmits its data using the small amount of harvested energy, the SU can help relay the primary data to improve the link robustness. Thus, the primary data can be more reliably delivered with less resource, and the SU can be awarded some resources for the spectrum sharing.
- The Alamouti coding technique [27] is adopted by the UE and the SU to simultaneously retransmit the

Yu *et al. EURASIP Journal on Wireless Communications and Networking* (2017) 2017:9

Page 3 of 13

primary data. Without requiring any extra bandwidth, the quality of primary data transmission can be improved.

- We analyze the success probabilities of transmission cases and then derive the throughput of both primary and secondary systems. The time allocation between EH and data transmission is investigated through maximizing the throughput of secondary system while guaranteeing the throughput of primary system.
- We investigate the impacts of various parameter settings to the system performance, such as the time allocation, the distances between different terminals, the transmission rate, and the transmission powers of terminals.

The rest of this paper is organized as follows. In Section 2, the energy and data cooperation-based spectrum sharing scheme is proposed. Section 3 explains the non-spectrum sharing model as a benchmark. In Section 4, we derive the throughput of both systems. Performance results are presented in Section 5. Section 6 concludes this paper.
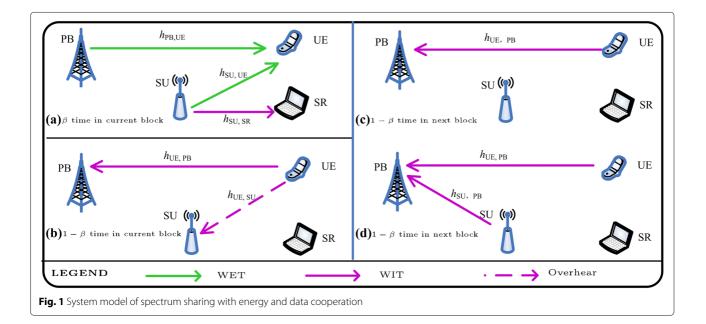
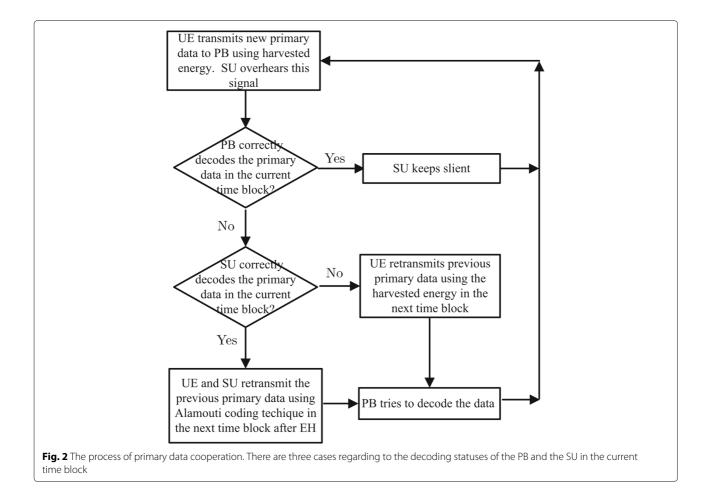## 2 Energy and data cooperation spectrum sharing

Figure 1 shows the system model of our proposed spectrum sharing, where a secondary link coexists with a primary link in the same geographic region. In the first β time, as shown in Fig. 1a, the PB transfers wireless energy to the UE, and meanwhile the SU communicates with the secondary receiver (SR). The secondary data transmission can be regarded as a source of energy that can be harvested by the UE. Since the energy signal transmitted by the PB is known to all the terminals, the SR can cancel this interference to decode its desired secondary data. With the secondary data transmission, the EH efficiency of the UE can be greatly improved, and thus more energy can be available for the primary data transmission. After the WET, as shown in Fig. 1b, the following $1 - \beta$ time is used for the uplink primary data transmission from the UE to the PB. At the same time, the SU will overhear the UE's signal and help relay the primary data in case the PB fails to decode it. As illustrated in Fig. 2, according to the decoding statuses of PB and SU, there are three possible transmission policies:

- If the PB correctly receives the primary data in the current block, a new primary data will be transmitted by the UE in the next block after the EH period.
- If both PB and SU erroneously receive the primary data in the current block, the UE will retransmit the primary data in the next block after the EH period, as shown in Fig. 1c.
- If the PB erroneously receives the primary data, but the SU correctly overhears it. The primary data will be retransmitted by UE and SU using the Alamouti coding technique in the next block after the EH period, as shown in Fig. 1d.

The primary data will be discarded if it is still incorrectly received by the PB after the retransmission. Each channel is assumed to undergo Rayleigh block fading, so the channel fading remains constant in one block, but varies independently from one block to another. The channels are assumed to consist of the small-scale fading and the large-scale path-loss, i.e., $h_{ij} = \chi_{ij} d_{ij}^{-\nu/2}$ ($i, j \in \{PB, UE, SU, SR\}$), where ν and d_{ij} denote the path-loss

Fig. 1 System model of spectrum sharing with energy and data cooperation

Fig. 2 The process of primary data cooperation. There are three cases regarding to the decoding statuses of the PB and the SU in the current time block

exponent and the distance between two terminals, respectively. The fading coefficient χ_{ij} is a circularly symmetric complex Gaussian random variable with unit variance. The channel gain $|h_{ij}|^2$ is exponentially distributed with the probability density function (PDF) $f_X(x) = \frac{1}{\lambda_{ij}}\exp(-\frac{x}{\lambda_{ij}})$, where $\mathbb{E}\{|h_{ij}|^2\} = \lambda_{ij} = d_{ij}^{-\nu}$. In each time block, the downlink and uplink channels are assumed to be reciprocal, i.e., the downlink energy transfer from PB and the uplink data transmission from UE suffers from the same channel fading, so $|h_{ij}|^2 = |h_{ji}|^2$. This assumption has been widely adopted in the literatures, such as [18] and [22]. In the cooperative transmission period, we assume that the locations of nodes do not change significantly [28]. The mathematical expectation is denoted as $\mathbb{E}\{\cdot\}$. The $(\cdot)^*$ and $(\cdot)^H$ represent complex conjugate and Hermitian transpose of matrix, respectively.

3 Benchmark primary system without spectrum sharing

In the non-spectrum sharing scenario, a PB intends to communicate with a UE. The PB has a continuous power supply, while the UE has to harvest the RF energy from the PB transmissions. This is actually the "Harvest-then-transmit" protocol as proposed in [18]. Each normalized time block consists of two phases. In the first θ time, the PB transfers energy to the UE over the downlink. In the remaining $(1-\theta)$ time, the UE transmits its data to the PB over the uplink using the harvested energy.

In the first θ time, the amount of energy harvested by the UE is denoted as $\mathbf{E}_u$ and given as [18, 26]

$$\mathbf{E}_u = \eta\theta p_b|h_{\text{PB,UE}}|^2, \tag{1}$$

where $\eta \in (0,1)$ represents the energy conversion efficiency and p_b denotes the transmit power of PB.

After harvesting energy in θ time, the primary data is transmitted from UE to PB in the remaining $1 - \theta$ time. The transmit power of UE is denoted as p_u^{no} and calculated as

$$p_u^{\text{no}} = \frac{\mathbf{E}_u}{1 - \theta}. \tag{2}$$

The achievable rate of primary link is expressed as

$$C_{\text{UE,PB}}^{\text{no}} = (1 - \theta) \log_2 \left(1 + \frac{p_u^{\text{no}}|h_{\text{UE,PB}}|^2}{\sigma^2}\right), \tag{3}$$

Yu *et al. EURASIP Journal on Wireless Communications and Networking* (2017) 2017:9

Page 5 of 13

where σ^2 represents the power of additive white Gaussian noise (AWGN) and it is the same at different receivers.

The throughput of primary system with non-spectrum sharing can be expressed as $\mathcal{V}_p = \Pr\{C_{UE,PB}^{no} \geq R_0\}R_0$. The primary data is assumed to be successfully received by PB if the channel achievable rate is no less than the fixed transmission rate R_0. The data success probability can be derived as

$$\Pr\left\{C_{UE,PB}^{no} \geq R_0\right\} = \exp\left(-\sqrt{\frac{(1-\theta)\rho_0\sigma^2}{\eta\theta p_b}}d_{UE,PB}^v\right),$$

(4)

where $\rho_0 = 2^{\frac{R_0}{1-\theta}} - 1$. The maximal throughput of the stand-alone primary network without spectrum sharing can be obtained via $\mathcal{V}_p^{max} = \max_{\beta\in(0,1)} \mathcal{V}_p$.

Since the UE is located far away from the PB, the EH efficiency is quite low due to the severe path-loss. Using the small amount of harvested energy, the primary data transmission is more likely to fail and the spectrum is wasted for the data retransmission.

4 Throughput of the spectrum sharing

In each normalized time block, the WET is performed in the first β fraction of time. The amount of energy harvested by the UE is denoted as E_{UE} and given as

$$E_{UE} = \eta\beta p_b|h_{PB,UE}|^2 + \eta\beta p_a|h_{SU,UE}|^2,$$

(5)

where p_a denotes the transmit power of the SU. The transmit power of the UE [1] can be expressed as

$$p_{UE} = \frac{E_{UE}}{1-\beta}.$$

(6)

After the WET, the UE transmits its own data to the PB in the remaining $1-\beta$ time, and the SU overhears the data from the UE. Based on the decoding status of UE and SU, there exists three transmission cases as follows:

- Case A: If the primary data is correctly received by the PB, the SU will keep silent.
- Case B: If both the PB and the SU erroneously receive the primary data, the primary data will be retransmitted in the next time block.
- Case C: If the primary data is erroneously received by the PB, but correctly decoded by the SU, the UE and the SU will simultaneously retransmit the primary data in the next time block using the Alamouti coding technique.

The total throughput of primary system includes the above three cases and it can be expressed as

$$\mathcal{L}_p = \left[\Pr(Suc, A) + \frac{1}{2}\Pr(Suc, B) + \frac{1}{2}\Pr(Suc, C)\right]R_0,$$

(7)

where the pre-factor $\frac{1}{2}$ accounts that one primary data packet is transmitted in the first time block, and it may be retransmitted in the following time block. The Suc means that the primary data is successfully delivered in a certain case.

4.1 Case A: original data transmission

In the primary data transmission, the achievable rate of the link between UE and PB is denoted as $C_{UE,PB}^{(1)}$ and given by

$$C_{UE,PB}^{(1)} = (1-\beta)\log_2\left(1 + \frac{p_{UE}|h_{UE,PB}|^2}{\sigma^2}\right),$$

(8)

where the pre-factor is applied because the primary data is broadcasted by the UE in $1-\beta$ time. The success probability of the original primary data transmission is expressed as $\Pr(Suc, A) = \Pr\left\{C_{UE,PB}^{(1)} \geq R_0\right\}$ and calculated as

$$\Pr(Suc, A) = \exp\left(-\sqrt{\frac{\rho_1}{a_1}}d_{UE,PB}^v\right) + d_{UE,PB}^v\int_0^{\sqrt{\frac{\rho_1}{a_1}}}\mathcal{I}_1(g_1)dg_1,$$

(9)

where $\rho_1 = 2^{\frac{R_0}{1-\beta}} - 1$, $a_1 = \frac{\beta}{1-\beta}\frac{\eta p_b}{\sigma^2}$, $a_2 = \frac{\beta}{1-\beta}\frac{\eta p_a}{\sigma^2}$, $g_1 = |h_{PB,UE}|^2$, and

$$\mathcal{I}_1(g_1) = \exp\left\{-\left[\frac{\rho_1 d_{SU,UE}^v}{a_2 g_1} + \left(d_{UE,PB}^v - \frac{a_1}{a_2}d_{SU,UE}^v\right)g_1\right]\right\}.$$

(10)

4.2 Case B: primary data retransmission from UE

For the primary data cooperation, the SU overhears the information transmitted from UE. The achievable rate between UE and SU in the current block is denoted as $C_{UE,SU}^{(1)}$ and given as

$$C_{UE,SU}^{(1)} = (1-\beta)\log_2\left(1 + \frac{p_{UE}|h_{UE,SU}|^2}{\sigma^2}\right).$$

(11)

If the primary data is erroneously received by both the PB and the SU in the second phase of the current time block, the UE will retransmit its data to the PB in the next time block, while the SU should keep silent. The achievable rate between UE and PB in the time block is denoted as $C_{UE,PB}^{(2)}$ and given as

$$C_{UE,PB}^{(2)} = (1-\beta)\log_2\left(1 + \frac{p_{UE}|\tilde{h}_{UE,PB}|^2}{\sigma^2}\right),$$

(12)

Yu *et al. EURASIP Journal on Wireless Communications and Networking* (2017) 2017:9

Page 6 of 13

where $\tilde{g}_1 = |\tilde{h}_{\text{UE,PB}}|^2$ represents the channel gain between UE and PB in the retransmission block.

The success probability of primary data transmission is denoted as $\text{Pr}(\text{Suc, B})$ and expressed as

$$\text{Pr}(\text{Suc, B}) = \text{Pr}\left\{C_{\text{UE,PB}}^{(1)} < R_0, C_{\text{UE,SU}}^{(1)} < R_0\right\}\text{Pr}\left\{C_{\text{UE,PB}}^{(2)} \geq R_0\right\}.$$

(13)

In Eq. (13), the first probability can be decomposed as

$$\text{Pr}\left\{C_{\text{UE,PB}}^{(1)} < R_0, C_{\text{UE,SU}}^{(1)} < R_0\right\}$$
$$= \underbrace{\text{Pr}\left\{g_1 < g_2, g_1 < \frac{\rho_1 - a_2 g_2^2}{a_1 g_2}\right\}}_{\mathcal{B}_a}$$
$$+ \underbrace{\text{Pr}\left\{g_1 \geq g_2, g_2 < \frac{\rho_1 - a_1 g_1^2}{a_1 g_2}\right\}}_{\mathcal{B}_b},$$

(14)

where $g_2 = |h_{\text{SU,UE}}|^2$. The results of the intermediate probability $\mathcal{B}_a$ and $\mathcal{B}_b$ are presented in Appendix I.

The second probability of (13) can be derived as

$$\text{Pr}\left\{C_{\text{UE,PB}}^{(2)} \geq R_0\right\} = \exp\left(-\sqrt{\frac{\rho_1}{a_1}}d_{\text{UE,PB}}^v\right)$$
$$+ d_{\text{UE,PB}}^v \int_0^{\sqrt{\frac{\rho_1}{a_1}}} \mathcal{I}_1(\tilde{g}_1)\text{d}\tilde{g}_1,$$

(15)

where $I_1(\tilde{g}_1)$ can be obtained according to (10).

4.3 Case C: cooperative data retransmission with Alamouti coding

After data transmission in the remaining $1 - \beta$ time, if the primary data is erroneously decoded by the PB, but correctly overheard by the SU, in the next time block, the UE and the SU will simultaneously retransmit the primary data using Alamouti coding scheme. The Alamouti coding scheme does not require channel state information at the transmitter side and can bring space diversity to improve the transmission robustness. The received signal at the PB can be expressed as [27]

$$\mathbf{Y} = \begin{bmatrix} y_1 \\ y_2 \end{bmatrix} = \begin{bmatrix} x_1 & x_2 \\ -x_2^* & x_1^* \end{bmatrix}\begin{bmatrix} \sqrt{p_{\text{UE}}}\tilde{h}_{\text{UE,PB}} \\ \sqrt{p_a}h_{\text{SU,PB}} \end{bmatrix} + \begin{bmatrix} n_1 \\ n_2 \end{bmatrix},$$

(16)

where n_1 and n_2 denote the AWGN with zero mean and variance σ^2. The signals from UE and SU are denoted as x_1 and x_2, respectively. In the next period, signal $-x_2^*$ is transmitted from UE and x_1^* is transmitted from SU, where $\mathbb{E}\{|x_1|^2\} = \mathbb{E}\{|x_2|^2\} = 1$.

The received signals at PB can be modeled as $\mathbf{y} = [y_1, y_2^*] = \mathbf{H}[x_1, x_2]^{\text{T}} + \mathbf{n}$, where $\mathbf{n}$ represents the noise

with unit power. The normalized channel matrix $\mathbf{H}$ can be written as

$$\mathbf{H} = \begin{bmatrix} \sqrt{\frac{p_{\text{UE}}}{\sigma^2}}\tilde{h}_{\text{UE,PB}} & \sqrt{\frac{p_a}{\sigma^2}}h_{\text{SU,PB}} \\ \sqrt{\frac{p_a}{\sigma^2}}h_{\text{SU,PB}}^* & -\sqrt{\frac{p_{\text{UE}}}{\sigma^2}}\tilde{h}_{\text{UE,PB}}^* \end{bmatrix}.$$

(17)

The achievable rate of the distributed Alamouti coding [29] can be calculated as

$$C_{\text{Alamouti}} = \frac{(1 - \beta)}{2}\log_2\left[\det\left(\mathbf{I} + \mathbf{H}\mathbf{H}^H\right)\right]$$
$$= (1 - \beta)\log_2\left(1 + \frac{p_{\text{UE}}}{\sigma^2}\tilde{g}_1 + \frac{p_a}{\sigma^2}g_3\right),$$

(18)

where $g_3 = |h_{\text{SU,PB}}|^2$ and $\mathbf{I}$ is the identity matrix.

If the primary data is erroneously received by PB, but it is correctly received by SU in the current time block, then UE and SU will use the Alamouti coding technique to simultaneously retransmit the primary data to PB in the second phase of the next time block. The success probability of primary data transmission is denoted as $\text{Pr}(\text{Suc, C})$ and calculated as

$$\text{Pr}(\text{Suc, C}) = \text{Pr}\left\{C_{\text{UE,PB}}^{(1)} < R_0, C_{\text{UE,SU}}^{(1)} \geq R_0\right\}\text{Pr}\left\{C_{\text{Alamouti}} \geq R_0\right\}.$$

(19)

In Eq. (19), the first probability can be calculated as

$$\text{Pr}\left\{C_{\text{UE,PB}}^{(1)} < R_0, C_{\text{UE,SU}}^{(1)} \geq R_0\right\}$$
$$= \underbrace{\text{Pr}\left\{g_2 < \frac{\rho_1 - a_1 g_1^2}{a_2 g_1}, g_2 > \sqrt{\frac{\rho_1}{a_2}}, g_1 < \sqrt{\frac{\rho_1}{a_1}}\right\}}_{\mathcal{F}_a}$$
$$+ \underbrace{\text{Pr}\left\{g_2 < \frac{\rho_1 - a_1 g_1^2}{a_2 g_1}, g_2 < \sqrt{\frac{\rho_1}{a_2}}, g_1 < \sqrt{\frac{\rho_1}{a_1}}\right\}}_{\mathcal{F}_b}$$
$$- \underbrace{\text{Pr}\left\{g_2 < \frac{\rho_1 - a_1 g_1^2}{a_2 g_1}, g_1 < \frac{\rho_1 - a_2 g_2^2}{a_1 g_2}, g_2 < \sqrt{\frac{\rho_1}{a_2}}, g_1 < \sqrt{\frac{\rho_1}{a_1}}\right\}}_{\mathcal{F}_c}.$$

(20)

The results of probabilities $\mathcal{F}_a$, $\mathcal{F}_b$, $\mathcal{F}_c$ are presented in Appendix II.

In Eq. (19), the second probability can be derived as

$$\text{Pr}\left\{C_{\text{Alamouti}} \geq R_0\right\}$$
$$= \underbrace{\text{Pr}\left\{\tilde{g}_1 < \sqrt{\frac{\rho_1}{a_1}}, g_2 > \frac{\rho_1 - b_1 g_3 - a_1 \tilde{g}_1^2}{a_2 g_1}, g_3 < \frac{\rho_1 - a_1 \tilde{g}_1^2}{b_1}\right\}}_{J_a}$$
$$+ \underbrace{\text{Pr}\left\{\tilde{g}_1 < \sqrt{\frac{\rho_1}{a_1}}, g_3 > \frac{\rho_1 - a_1 \tilde{g}_1^2}{b_1}\right\}}_{J_b} + \underbrace{\text{Pr}\left\{\tilde{g}_1 \geq \sqrt{\frac{\rho_1}{a_1}}\right\}}_{J_c},$$

(21)

where $b_1 = \frac{p_a}{\sigma^2}$. The probabilities J_a, J_b and J_c are derived as

$$
\begin{aligned}
J_a = d_{\text{UE,PB}}^v \int_0^{\sqrt{\frac{\rho_1}{a_1}}} &\exp\left[-\left(\frac{\rho_1 - a_1\tilde{g}_1^2}{a_2\tilde{g}_1}d_{\text{SU,UE}}^v + d_{\text{UE,PB}}^v\tilde{g}_1\right)\right] \\
&\times \left(\frac{a_2\tilde{g}_1}{a_2\tilde{g}_1 - b_1 d_{\text{SU,UE}}^v d_{\text{SU,PB}}^{-v}}\right) \\
&\times \left\{1 - \exp\left[-\left(d_{\text{SU,PB}}^v - \frac{b_1 d_{\text{SU,UE}}^v}{a_2\tilde{g}_1}\right)\frac{\rho_1 - a_1\tilde{g}_1^2}{b_1}\right]\right\} d\tilde{g}_1.
\end{aligned}
\tag{22}
$$

$$
\begin{aligned}
J_b &= d_{\text{UE,PB}}^v \int_0^{\sqrt{\frac{\rho_1}{a_1}}} \exp\left[-\left(\frac{\rho_1}{b_1}d_{\text{SU,PB}}^v + \tilde{g}_1 d_{\text{UE,PB}}^v - \frac{a_1\tilde{g}_1^2}{b_1}d_{\text{SU,PB}}^v\right)\right] d\tilde{g}_1 \\
&= \frac{d_{\text{UE,PB}}^v}{2}\sqrt{\frac{\pi b_1}{a_1 d_{\text{SU,PB}}^v}}\exp\left(-\frac{4a_1\rho_1 d_{\text{SU,PB}}^{2v} + b_1^2 d_{\text{UE,PB}}^{2v}}{4a_1 d_{\text{SU,PB}}^v b_1}\right) \\
&\quad \times \left[\text{erfi}\left(\sqrt{\frac{a_1 d_{\text{SU,PB}}^v}{b_1}}\tilde{g}_1 - \frac{d_{\text{UE,PB}}^v}{2\sqrt{\frac{a_1 d_{\text{SU,PB}}^v}{b_1}}}\right)\right]_0^{\sqrt{\frac{\rho_1}{a_1}}},
\end{aligned}
\tag{23}
$$

where $erfi(z) = \frac{\text{erf}(iz)}{i}$ and the error function $\text{erf}(x) = \frac{2}{\sqrt{\pi}}\int_0^x e^{-t^2}\,dt$. Eq. (23) can be solved via ([30], (2.325.13)).

$$
J_c = \exp\left(-\sqrt{\frac{(1-\beta)\rho_1\sigma^2}{\beta\eta p_b}}d_{\text{UE,PB}}^v\right).
\tag{24}
$$

Substituting (22), (23), and (24) into (21), the success probability of primary data retransmission using Alamouti coding, which is the second probability of (19), can be obtained. According to (19), the success probability of primary data transmission can be obtained.

4.4 Throughput of secondary system

The secondary data is transmitted from SU to SR in each time block with time fraction β. Since the energy signals are well known by all the terminals, and the SR knows the perfect channel state information (CSI) towards the PB, the SR will retrieve its desired signal through canceling the primary energy signal firstly. This assumption has been widely used in the literatures using the successive interference cancelation technique, such as [10, 31]. The achievable rate of secondary link is expressed as:

$$
C_{\text{SU,SR}} = \beta \log_2\left(1 + \frac{p_a|h_{\text{SU,SR}}|^2}{\sigma^2}\right).
\tag{25}
$$

The throughput of secondary system can be given as $\mathcal{L}_s = \Pr\{C_{\text{SU,SR}} \geq R_1\}R_1$, where $\Pr\{C_{\text{SU,SR}} \geq R_1\}$ represents the success probability of secondary data transmission and R_1 denotes the transmission rate of secondary

link. The success probability of secondary data transmission can be derived as

$$
\Pr\{C_{\text{SU,SR}} \geq R_1\} = \exp\left(-\frac{\rho_2\sigma^2}{p_a d_{\text{SU,SR}}^{-v}}\right),
\tag{26}
$$

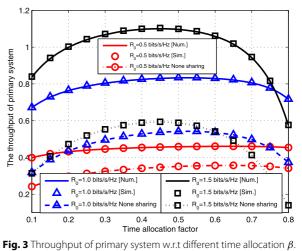where $\rho_2 = 2^{\frac{R_1}{\beta}} - 1$.

5 Numerical and simulation results

In this section, the simulation results are presented to validate our analysis. The impacts of various parameter settings, such as the time allocation, the distances between terminals, the transmission rates, and the transmission powers, to the system performance are revealed. Unless stated otherwise, the system general parameters are set as the noise power $N_0 = -80$ dBw, the energy conversion efficiency $\eta = 0.8$, the path-loss exponent $v = 3$, the transmission power of PB $p_b = -10$ dBw, the transmission power of SU $p_a = -20$ dBw, and the transmission rate $R_0 = 1$ bits/s/Hz.

5.1 Validate the analytical results

With the variation of system parameters, the decoding status of UE or SU will be changed from one case to another. The total throughput of primary system, as shown in Eq. (7), includes the throughput of Case A, Case B, and Case C together, which have been analyzed in Section 4. We will validate the analytical results using Monte Carlo simulations.

Figure 3 shows the throughput of primary system with respect to (w.r.t.) β for different R_0. With the increase of β, the throughput of primary system increases until reaching the maximal value and then deteriorates. The time allocation factor directly affects the throughput of primary system. The smaller the value of β, the less energy

Fig. 3 Throughput of primary system w.r.t different time allocation β. The parameters are set as $d_{\text{PB,UE}} = 10$m, $d_{\text{SU,UE}} = 5$ m and $d_{\text{SU,PB}} = 6$ m
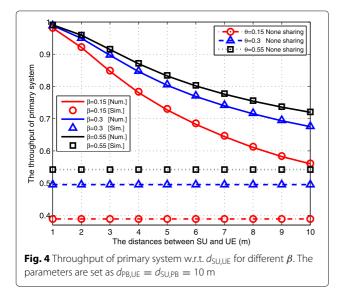
is harvested by UE, which is detrimental to the uplink data transmission. But, on the other hand, the smaller β is beneficial for the primary data transmission as it lasts for a longer time. Moreover, with the increase of the transmission rate of primary data, the throughput of primary system gets better.
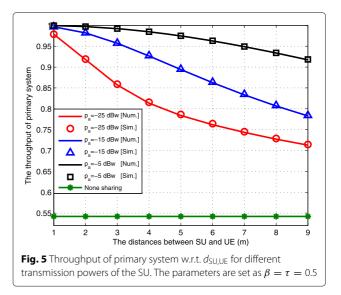
Figure 4 shows the throughput of primary system w.r.t. the distance between SU and UE for different β. In the simulations, the PB is located at the center of a disk, then the locations of UE and SU vary on the edge of the circle, which means $d_{PB,UE}$ and $d_{SU,PB}$ are the radius of this disk. For different β, the throughput of primary system deteriorates with the prolongation of $d_{SU,UE}$, because the longer the distance, the worse the average channel quality.

Figure 5 shows the throughput of primary system w.r.t. the distance between SU and UE for different transmission powers of SU. The distances are set as $d_{SU,PB} = d_{PB,UE} - d_{SU,UE}$. With the energy assistance from SU, the UE will harvest more energy to support the wireless information transfer (WIT), thereby, the throughput of primary system gets larger with the increase of p_a. Furthermore, even if adding up the p_a, the throughput of primary system still becomes worse with the increase of $d_{SU,UE}$.

Figure 6 shows the throughput of primary system w.r.t. the transmission power of SU for different β. The throughput of primary system improves when the transmission power of SU gets larger from -30 dBw to 0 dBw. In this figure, we can observe that with the energy assistance of SU, the throughput of primary system can be significantly increased, because more energy can be harvested by UE for the data transmission.

From Figs. 3 to 6, it can be seen that our theoretical results coincide exactly with the simulation results, which can verify the tightness of our analysis. Moreover,
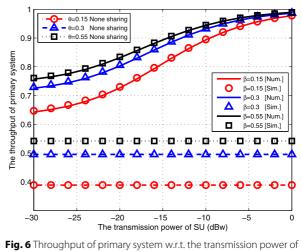

Fig. 5 Throughput of primary system w.r.t. $d_{SU,UE}$ for different transmission powers of the SU. The parameters are set as $\beta = \tau = 0.5$

our proposed scheme can greatly improve the throughput compared with the none spectrum sharing.
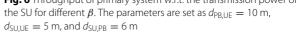
5.2 Maximal throughput of secondary system

We aim to maximize the throughput of secondary system, while guaranteeing that the throughput of primary system should not be degraded compared with the non-spectrum sharing model. The optimization problem can be formulated as

$$\max_{\beta \in (0,1)} \quad \mathcal{L}_s$$
$$\text{s. t.} \quad \mathcal{L}_p \geq \mathcal{V}_p^{\max}, \tag{27}$$

where $\mathcal{L}_p$ and $\mathcal{L}_s$ represent the throughput of primary system and secondary system, respectively, in the cooperative
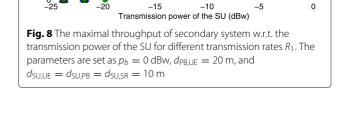

Fig. 4 Throughput of primary system w.r.t. $d_{SU,UE}$ for different β. The parameters are set as $d_{PB,UE} = d_{SU,PB} = 10$ m

Fig. 6 Throughput of primary system w.r.t. the transmission power of the SU for different β. The parameters are set as $d_{PB,UE} = 10$ m, $d_{SU,UE} = 5$ m, and $d_{SU,PB} = 6$ m

Yu *et al. EURASIP Journal on Wireless Communications and Networking* (2017) 2017:9

Page 9 of 13

spectrum sharing. $\mathcal{V}_p^{\max}$ denotes the maximal throughput of the stand-alone primary network without spectrum sharing.

As shown in (9), (13), and (19), the throughput expressions of primary system are complicated w.r.t. the power allocation factor. The closed-form solution of the optimal β is not available, but it can be numerically determined according to the optimization problem (27) through the one dimensional search in (0, 1).

Figure 7 depicts the maximal throughput of secondary system w.r.t. $d_{SU,UE}$ for different transmission rates R_0. The distance between SU and PB varies on $d_{SU,PB} = d_{PB,UE} - d_{SU,UE}$. We can see that the maximal throughput of secondary system gets smaller with the increase of $d_{SU,UE}$ and R_0. The smaller R_0 is beneficial to improve the performance of secondary system as more resources can be allocated for the secondary data transmission.

Figure 8 shows the maximal throughput of secondary system w.r.t. the transmission power of SU for different transmission rates R_1. The maximal throughput of secondary system improves dramatically with the increase of the transmission power of SU and R_1. The reason is that, with the increase of the transmission power of SU, the primary throughput constraint can be easily satisfied and more resources can be allocated for the secondary data transmission, thereby, the success probability tends to be 1. As a result, the maximal throughput of secondary system will gradually approach the value of R_1.

Figure 9 shows the maximal throughput of secondary system w.r.t. the transmission rate R_1 for different $d_{SU,SR}$. The throughput of secondary system gets better first and then turns worse with the increase of R_1. The reason is that with the increase of R_1, the success probability of secondary system will decrease and then the maximal

Fig. 8 The maximal throughput of secondary system w.r.t. the transmission power of the SU for different transmission rates R_1. The parameters are set as $p_b = 0$ dBw, $d_{PB,UE} = 20$ m, and $d_{SU,UE} = d_{SU,PB} = d_{SU,SR} = 10$ m
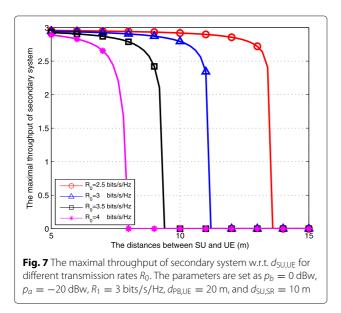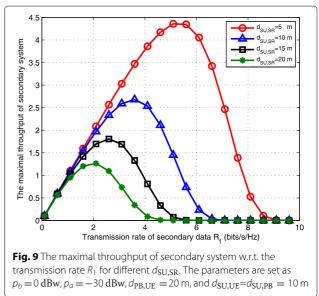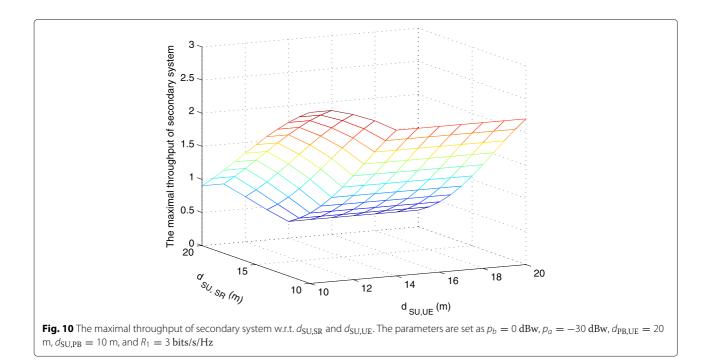
throughput of secondary system becomes worse. Furthermore, the throughput gets smaller when the SU is departed far away from the SR.

Figure 10 shows the maximal throughput of secondary system w.r.t. $d_{SU,SR}$ and $d_{SU,UE}$. With the increase of $d_{SU,SR}$, the average channel quality becomes worse, so the maximal throughput of secondary system gets smaller. When the SU is departed far away from the UE, the efficiency of WET becomes worse, so less energy will be harvested by the UE. In this case, less time will be allocated to the WET to satisfy the primary throughput
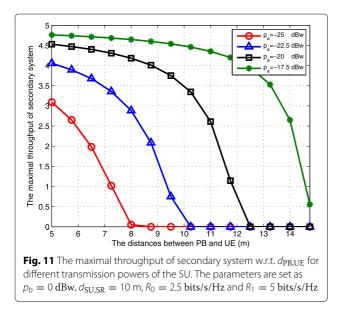

Fig. 7 The maximal throughput of secondary system w.r.t. $d_{SU,UE}$ for different transmission rates R_0. The parameters are set as $p_b = 0$ dBw, $p_a = -20$ dBw, $R_1 = 3$ bits/s/Hz, $d_{PB,UE} = 20$ m, and $d_{SU,SR} = 10$ m

Fig. 9 The maximal throughput of secondary system w.r.t. the transmission rate R_1 for different $d_{SU,SR}$. The parameters are set as $p_b = 0$ dBw, $p_a = -30$ dBw, $d_{PB,UE} = 20$ m, and $d_{SU,UE} = d_{SU,PB} = 10$ m

Yu *et al. EURASIP Journal on Wireless Communications and Networking* (2017) 2017:9

Page 10 of 13

Fig. 10 The maximal throughput of secondary system w.r.t. $d_{SU,SR}$ and $d_{SU,UE}$. The parameters are set as $p_b = 0$ dBw, $p_a = -30$ dBw, $d_{PB,UE} = 20$ m, $d_{SU,PB} = 10$ m, and $R_1 = 3$ bits/s/Hz

constraint. As a result, the maximal throughput of secondary system gets smaller and then stays almost constant with the further increase of $d_{SU,UE}$.

Figure 11 shows the maximal throughput of secondary system w.r.t. $d_{PB,UE}$ for different transmission powers of the SU. The SU is located at the center between PB and UE. We can see that the maximal throughput of secondary system gets worse when $d_{PB,UE}$ grows steadily and the transmission power of SU goes down. With the increase of $d_{PB,UE}$, the throughput of primary system deteriorates and thus more resource will be allocated to meet the primary

throughput constraint. On the another hand, the maximal throughput will be decreased with the declining of p_a.

6 Conclusions

In this paper, we have proposed an energy-harvesting-based spectrum sharing scheme, where the secondary user can transmit its own data along with the energy signal transmission from the primary base station. The interference of secondary data transmission can help improve the energy harvesting efficiency of primary user. Apart from the energy cooperation, the secondary user can also help the primary data relaying, where the Alamouti coding technique is adopted to simultaneously retransmit the primary data. Through using the energy to exchange for the spectrum by the secondary user, the transmission requirements of both systems can be well accommodated.

In the future, there are several interesting directions. Firstly, when the numbers of SU vary with time, this system model can be extended to the multiple SUs scenario. The SU scheduling algorithms should be designed by considering channel conditions. Secondly, the interference management and mode selection can be studied for the smart devices equipped with multiple antennas or radio interfaces (e.g., Wi-Fi, LTE, WiMAX, Bluetooth, etc.) [32, 33]; Thirdly, various coding schemes can be designed to improve the transmission rate and reliability, such as Raptor code for wireless video transmission [34].

Endnote

[1] To realize the spectrum sharing, there need some coordinations between PB, UE and SU by exchanging

Fig. 11 The maximal throughput of secondary system w.r.t. $d_{PB,UE}$ for different transmission powers of the SU. The parameters are set as $p_b = 0$ dBw, $d_{SU,SR} = 10$ m, $R_0 = 2.5$ bits/s/Hz and $R_1 = 5$ bits/s/Hz

Yu *et al. EURASIP Journal on Wireless Communications and Networking*   (2017) 2017:9

Page 11 of 13

the control signals. In this process, the PB, UE and SU may consume some energy and time, which is negligible compared with the long-time data transmission [35].

Appendix I: derivation of (14)

In Eq. (14), the intermediate probability $\mathcal{B}_a$ is derived as

$$
\begin{aligned}
\mathcal{B}_a = {} & 1 - \exp\left(-\sqrt{\frac{\rho_1}{a_2}} d^v_{\text{SU,UE}}\right) \\
& - \frac{d^v_{\text{SU,UE}}}{w_1}\left[1 - \exp\left(-w_1\sqrt{\frac{\rho_1}{a_1+a_2}}\right)\right] \\
& - d^v_{\text{SU,UE}} \int_{\sqrt{\frac{\rho_1}{a_1+a_2}}}^{\sqrt{\frac{\rho_1}{a_2}}} \mathcal{I}_2(g_2) \mathrm{d}g_2,
\end{aligned}
\tag{28}
$$

where $w_1 = d^v_{\text{UE,PB}} + d^v_{\text{SU,UE}}$, and

$$
\mathcal{I}_2(g_2) = \exp\left\{-\left[\frac{\rho_1 d^v_{\text{UE,PB}}}{a_1 g_2} + \left(d^v_{\text{SU,UE}} - \frac{a_2 d^v_{\text{UE,PB}}}{a_1}\right)g_2\right]\right\}.
\tag{29}
$$

In Eq. (14), the intermediate probability $\mathcal{B}_b$ is derived as

$$
\begin{aligned}
\mathcal{B}_b = {} & 1 - \exp\left(-\sqrt{\frac{\rho_1}{a_1}} d^v_{\text{UE,PB}}\right) - d^v_{\text{UE,PB}} \int_{\sqrt{\frac{\rho_1}{a_1+a_2}}}^{\sqrt{\frac{\rho_1}{a_1}}} \mathcal{I}_1(g_1) \mathrm{d}g_1 \\
& - \frac{d^v_{\text{UE,PB}}}{w_1}\left[1 - \exp\left(-w_1\sqrt{\frac{\rho_1}{a_1+a_2}}\right)\right],
\end{aligned}
\tag{30}
$$

where $I_1(g_1)$ is given in (10).

In Eq. (13), the post-intermediate probability can be calculated as

$$
\Pr\left\{C^{(2)}_{\text{UE,PB}} \geq R_0\right\} = \exp\left(-\sqrt{\frac{\rho_1}{a_1}} d^v_{\text{UE,PB}}\right) \\
+ d^v_{\text{UE,PB}} \int_0^{\sqrt{\frac{\rho_1}{a_1}}} \mathcal{I}_1(g_1) \mathrm{d}g_1.
\tag{31}
$$

Substituting the results of (14) and (31) into (13), we can obtain the success probability of the primary data retransmission from the UE.

Appendix II: derivation of (20)

The intermediate probability $\mathcal{F}_a$ in Eq. (20) is zero if $\sqrt{\frac{\rho_1}{a_2}} \geq \frac{\rho_1 - a_1 g_1^2}{a_2 g_1}$, otherwise, $\mathcal{F}_a$ can be derived as

$$
\begin{aligned}
\mathcal{F}_a = {} & \exp\left(-\sqrt{\frac{\rho_1}{a_2}} d^v_{\text{SU,UE}}\right)\left\{1 - \exp\left[-\min\left(\sqrt{\frac{\rho_1}{a_1}}, q\right) d^v_{\text{UE,PB}}\right]\right\} \\
& - d^v_{\text{UE,PB}} \int_0^{\min\left(\sqrt{\frac{\rho_1}{a_1}}, q\right)} \mathcal{I}_1(g_1) \mathrm{d}g_1,
\end{aligned}
\tag{32}
$$

where $q = \frac{-\sqrt{a_2\rho_1} + \sqrt{a_2\rho_1 + 4a_1\rho_1}}{2a_1}$ and $I_1(g_1)$ is given in (10).

In Eq. (20), the intermediate probability $\mathcal{F}_b$ is

$$
\begin{aligned}
\mathcal{F}_b = {} & \underbrace{\Pr\left\{g_1 < \min\left(\sqrt{\frac{\rho_1}{a_1}}, q\right), g_2 < \sqrt{\frac{\rho_1}{a_2}}\right\}}_{\mathcal{F}_{b1}} \\
& + \underbrace{\Pr\left\{g_1 > q, g_1 < \sqrt{\frac{\rho_1}{a_1}}, g_2 < \frac{\rho_1 - a_1 g_1^2}{a_2 g_1}\right\}}_{\mathcal{F}_{b2}}.
\end{aligned}
\tag{33}
$$

In Eq. (33), the intermediate probability $\mathcal{F}_{b1}$ is

$$
\begin{aligned}
\mathcal{F}_{b1} = {} & \left\{1 - \exp\left[-\min\left(\sqrt{\frac{\rho_1}{a_1}}, q\right) d^v_{\text{UE,PB}}\right]\right\} \\
& \left[1 - \exp\left(-\sqrt{\frac{\rho_1}{a_2}} d^v_{\text{SU,UE}}\right)\right].
\end{aligned}
\tag{34}
$$

If $q \geq \sqrt{\frac{\rho_1}{a_1}}$, $\mathcal{F}_{b2}$ equals zero, otherwise, the intermediate probability $\mathcal{F}_{b2}$ in expression (33) can be calculated as

$$
\begin{aligned}
\mathcal{F}_{b2} = {} & \exp(-q d^v_{\text{UE,PB}}) - \exp\left(-\sqrt{\frac{\rho_1}{a_1}} d^v_{\text{UE,PB}}\right) \\
& - d^v_{\text{UE,PB}} \int_q^{\sqrt{\frac{\rho_1}{a_1}}} \mathcal{I}_1(g_1) \mathrm{d}g_1.
\end{aligned}
\tag{35}
$$

Substituting (34) and (35) into (33), the intermediate probability $\mathcal{F}_b$ can be obtained.

In Eq. (20), the intermediate probability $\mathcal{F}_c$ is

$$
\begin{aligned}
\mathcal{F}_c = {} & \underbrace{\Pr\left\{g_1 < g_2, g_1 < \frac{\rho_1 - a_2 g_2^2}{a_1 g_2}, g_2 < \sqrt{\frac{\rho_1}{a_2}}, g_1 < \sqrt{\frac{\rho_1}{a_1}}\right\}}_{\mathcal{F}_{c1}} \\
& + \underbrace{\Pr\left\{g_1 \geq g_2, g_2 < \frac{\rho_1 - a_1 g_1^2}{a_2 g_1}, g_2 < \sqrt{\frac{\rho_1}{a_2}}, g_1 < \sqrt{\frac{\rho_1}{a_1}}\right\}}_{\mathcal{F}_{c2}},
\end{aligned}
\tag{36}
$$

where $\mathcal{F}_{c1}$ and $\mathcal{F}_{c2}$ can be derived in the following.

$$
\begin{aligned}
\mathcal{F}_{c1} = {} & \underbrace{\Pr\left\{g_1 < g_2, g_2 < \sqrt{\frac{\rho_1}{a_1+a_2}}\right\}}_{\mathcal{F}_{c11}} \\
& + \underbrace{\Pr\left\{g_1 < \frac{\rho_1 - a_2 g_2^2}{a_1 g_2}, \sqrt{\frac{\rho_1}{a_1+a_2}} < g_2 < \sqrt{\frac{\rho_1}{a_2}}, g_2 > q_1\right\}}_{\mathcal{F}_{c12}} \\
& + \underbrace{\Pr\left\{g_1 < \sqrt{\frac{\rho_1}{a_1}}, \sqrt{\frac{\rho_1}{a_1+a_2}} < g_2 < \sqrt{\frac{\rho_1}{a_2}}, g_2 < q_1\right\}}_{\mathcal{F}_{c13}}.
\end{aligned}
\tag{37}
$$

where $q_1 = \frac{-\sqrt{a_1\rho_1} + \sqrt{a_1\rho_1 + 4a_2\rho_1}}{2a_2}$.

The intermediate probability $\mathcal{F}_{c11}$, $\mathcal{F}_{c12}$ and $\mathcal{F}_{c13}$ in (37) can be derived as

$$\mathcal{F}_{c11} = 1 - \exp\left(-\sqrt{\frac{\rho_1}{a_1+a_2}}d_{\text{SU,UE}}^{v}\right)$$
$$- \frac{d_{\text{SU,UE}}^{v}}{w_1}\left[1 - \exp\left(-w_1\sqrt{\frac{\rho_1}{a_1+a_2}}\right)\right]. \quad (38)$$

If $\sqrt{\frac{\rho_1}{a_2}} \leq \max\left(\sqrt{\frac{\rho_1}{a_1+a_2}}, q_1\right)$, the $\mathcal{F}_{c12}$ is zero, otherwise, $\mathcal{F}_{c12}$ can be derived as

$$\mathcal{F}_{c12} = \exp\left[-\max\left(\sqrt{\frac{\rho_1}{a_1+a_2}}, q_1\right)d_{\text{SU,UE}}^{v}\right]$$
$$- \exp\left(-\sqrt{\frac{\rho_1}{a_2}}d_{\text{SU,UE}}^{v}\right)$$
$$- d_{\text{SU,UE}}^{v}\int_{\max\left(\sqrt{\frac{\rho_1}{a_1+a_2}}, q_1\right)}^{\sqrt{\frac{\rho_1}{a_2}}}\mathcal{I}_2(g_2)\mathrm{d}g_2, \quad (39)$$

where $I_2(g_2)$ is given in (29).

If $\min\left(\sqrt{\frac{\rho_1}{a_2}}, q_1\right) \leq \sqrt{\frac{\rho_1}{a_1+a_2}}$, $\mathcal{F}_{c13}$ equals zero, otherwise, $\mathcal{F}_{c13}$ is obtained as

$$\mathcal{F}_{c13} = \left[1 - \exp\left(-\sqrt{\frac{\rho_1}{a_1}}d_{\text{UE,PB}}^{v}\right)\right]\left\{\exp\left(-\sqrt{\frac{\rho_1 d_{\text{SU,UE}}^{2v}}{a_1+a_2}}\right)\right.$$
$$\left. -\exp\left[-\min\left(\sqrt{\frac{\rho_1}{a_2}}, q_1\right)d_{\text{SU,UE}}^{v}\right]\right\}. \quad (40)$$

Substituting (38), (39), and (40) into (37), the intermediate probability $\mathcal{F}_{c1}$ can be obtained.

In Eq. (36), the intermediate probability $\mathcal{F}_{c2}$ is

$$\mathcal{F}_{c2} = \underbrace{\Pr\left\{g_2 < g_1, g_1 < \sqrt{\frac{\rho_1}{a_1+a_2}}\right\}}_{\mathcal{F}_{c21}}$$
$$+ \underbrace{\Pr\left\{g_2 < \frac{\rho_1 - a_1 g_1^2}{a_2 g_1}, \sqrt{\frac{\rho_1}{a_1+a_2}} < g_1 < \sqrt{\frac{\rho_1}{a_1}}, g_1 > q\right\}}_{\mathcal{F}_{c22}}$$
$$+ \underbrace{\Pr\left\{g_2 < \sqrt{\frac{\rho_1}{a_2}}, g_1 > \sqrt{\frac{\rho_1}{a_1+a_2}}, g_1 < \sqrt{\frac{\rho_1}{a_1}}, g_1 < q\right\}}_{\mathcal{F}_{c23}}. \quad (41)$$

The intermediate probability $\mathcal{F}_{c21}$, $\mathcal{F}_{c22}$ and $\mathcal{F}_{c23}$ in (41) can be derived as:

$$\mathcal{F}_{c21} = 1 - \exp\left(-\sqrt{\frac{\rho_1}{a_1+a_2}}d_{\text{UE,PB}}^{v}\right)$$
$$- \frac{d_{\text{UE,PB}}^{v}}{w_1}\left[1 - \exp\left(-w_1\sqrt{\frac{\rho_1}{a_1+a_2}}\right)\right]. \quad (42)$$

If $\sqrt{\frac{\rho_1}{a_1}} \leq \max\left(\sqrt{\frac{\rho_1}{a_1+a_2}}, q\right)$, the intermediate probability $\mathcal{F}_{c22}$ in Eq. (41) is zero, otherwise, $\mathcal{F}_{c22}$ can be expressed as

$$\mathcal{F}_{c22} = \exp\left[-\max\left(\sqrt{\frac{\rho_1}{a_1+a_2}}, q\right)d_{\text{UE,PB}}^{v}\right]$$
$$- \exp\left(-\sqrt{\frac{\rho_1}{a_1}}d_{\text{UE,PB}}^{v}\right)$$
$$- d_{\text{UE,PB}}^{v}\int_{\max\left(\sqrt{\frac{\rho_1}{a_1+a_2}}, q\right)}^{\sqrt{\frac{\rho_1}{a_1}}}\mathcal{I}_1(g_1)\mathrm{d}g_1. \quad (43)$$

If $\sqrt{\frac{\rho_1}{a_1+a_2}} \geq \min\left(\sqrt{\frac{\rho_1}{a_1}}, q\right)$, the $\mathcal{F}_{c23}$ is zero, otherwise, the $\mathcal{F}_{c23}$ is

$$\mathcal{F}_{c23} = \left[1 - \exp\left(-\sqrt{\frac{\rho_1 d_{\text{SU,UE}}^{2v}}{a_2}}\right)\right]\left\{\exp\left(-\sqrt{\frac{\rho_1 d_{\text{UE,PB}}^{2v}}{a_1+a_2}}\right)\right.$$
$$\left. -\exp\left[-\min\left(\sqrt{\frac{\rho_1}{a_1}}, q\right)d_{\text{UE,PB}}^{v}\right]\right\}. \quad (44)$$

Substituting (42), (43), and (44) into (41), the intermediate probability $\mathcal{F}_{c2}$ can be obtained. Summarizing (32), (33), and (36), the first probability of (20) can be obtained.

References
1. NB Carvalho, A Georgiadis, A Costanzo, H Rogier, A Collado, JA García, S Lucyszyn, et al., Wireless power transmission: R&D activities within Europe. IEEE Trans. Microw. Theory Tech. **62**(4), 1031–1045 (2014)
2. AM Zungeru, LM Ang, S Prabaharan, KP Seng, *Radio frequency energy harvesting and management for wireless sensor networks, Green Mobile Devices and Networks: Energy Optimization and Scavenging Techniques.* (CRC Press, Boca Raton, 2012), pp. 341–368
3. I Krikidis, Simultaneous information and energy transfer in large-scale networks with/without relaying. IEEE Trans. Commun. **62**(3), 900–912 (2014)
4. S Ulukus, A Yener, E Erkip, O Simeone, M Zorzi, P Grover, K Huang, Energy harvesting wireless communications: A review of recent advances. IEEE J. Sel. Areas Commun. **33**(3), 360–381 (2015)
5. M Gorlatova, A Wallwater, G Zussman, Networking low-power energy harvesting devices: measurements and algorithms. IEEE Trans. Mobile Comput. **12**(9), 1853–1865 (2013)
6. Powercast, Power harvester brochure. http://www.powercastco.com/products/powerharvester-receivers/. Accessed 7 June 2015
7. C Song, Y Huang, J Zhou, J Zhang, S Yuan, P Carter, A High-efficiency broadband rectenna for ambient wireless energy harvesting. IEEE Trans. Antennas Propag. **63**(8), 3486–3495 (2015)

8.   Y Han, A Pandharipande, SH Ting, Cooperative decode-and-forward relaying for secondary spectrum access. IEEE Trans. Wireless Commun. **8**(10), 4945–4950 (2009)

9.   K Huang, VKN Lau, Y Chen, Spectrum sharing between cellular and mobile ad hoc networks: transmission capacity trade-off. IEEE J. Sel. Areas Commun. **27**(7), 1256–1267 (2009)

10.   Y Han, SH Ting, A Pandharipande, Cooperative spectrum sharing protocol with secondary user selection. IEEE Trans. Wireless Commun. **9**(9), 2914–2923 (2010)

11.   W Su, JD Matyjas, S Batalama, Active cooperation between primary users and cognitive radio users in heterogeneous ad-hoc networks. IEEE Trans. Signal Process. **60**(4), 1796–1805 (2012)

12.   C Zhai, W Zhang, PC Ching, Cooperative Spectrum sharing based on two-path successive relaying. IEEE Trans. Commun. **61**(6), 2260–2270 (2013)

13.   X Zhou, R Zhang, CK Ho, Wireless information and power transfer: architecture design and rate-energy tradeoff. IEEE Trans. Commun. **61**(11), 4754–4767 (2013)

14.   DWK Ng, ES Lo, R Schober, Wireless information and power transfer: energy efficiency optimization in OFDMA systems. IEEE Trans. Wireless Commun. **12**(12), 6352–6370 (2013)

15.   K Huang, E Larsson, Simultaneous information and power transfer for broadband wireless systems. IEEE Trans. Signal Process. **61**(23), 5972–5986 (2013)

16.   C Zhai, J Liu, Cooperative wireless energy harvesting and information transfer in stochastic networks. EURASIP J. Wireless Commun. and Network. **2015**(44), 1–22 (2015)

17.   J Rubio, A Pascual-Iserte, in *Proc.of IEEE Global, Communications Conference (GLOBECOM)*. Simultaneous wireless information and power transfer in multiuser MIMO systems (IEEE, Atlanta, 2013), pp. 2755–2760

18.   H Ju, R Zhang, Throughput maximization in wireless powered communication networks. IEEE Trans. Wireless Commun. **13**(1), 418–428 (2014)

19.   K Huang, VKN Lau, Enabling wireless power transfer in cellular networks: architecture, modeling and deployment. IEEE Trans. Wireless Commun. **13**(2), 902–912 (2014)

20.   S Park, J Heo, B Kim, W Chung, H Wang, D Hong, in *Proc.of IEEE 23rd, International Symposium on Personal Indoor and Mobile Radio Communications (PIMRC)*. Optimal mode selection for cognitive radio sensor networks with RF energy harvesting (IEEE, Sydney, 2012), pp. 2155–2159

21.   S Lee, R Zhang, K Huang, Opportunistic wireless energy harvesting in cognitive radio networks. IEEE Trans. Wireless Commun. **12**(9), 4788–4799 (2013)

22.   SA Mousavifar, Y Liu, C Leung, M Elkashlan, TQ Duong, in *Proc.of IEEE 80th. Vehicular, Technology Conference (VTC Fall)*. Wireless energy harvesting and spectrum sharing in cognitive radio (IEEE, Vancouver, 2014), pp. 1–5

23.   G Zheng, Z Ho, EA Jorswieck, B Ottersten, Information and energy cooperation in cognitive radio networks. IEEE Trans. Signal Process. **62**(9), 2290–2303 (2014)

24.   DT Hoang, D Niyato, P Wang, DI Kim, Opportunistic channel access and RF energy harvesting in cognitive radio networks. IEEE J. Sel. Areas Commun. **32**(11), 2039–2052 (2014)

25.   S Park, D Hong, Achievable throughput of energy harvesting cognitive radio networks. IEEE Trans. Wireless Commun. **13**(2), 1010–1022 (2014)

26.   H Chen, Y Li, JL Rebelatto, BF Uchôa-Filho, B Vucetic, Harvest-then-cooperate: wireless-powered cooperative communications. IEEE Trans. Signal Process. **63**(7), 1700–1711 (2015)

27.   SM Alamouti, A simple transmit diversity technique for wireless communications. IEEE J. Sel. Areas Commun. **16**(8), 1451–1458 (1998)

28.   L Xiong, L Libman, G Mao, Uncoordinated cooperative communications in highly dynamic wireless networks. IEEE J. Sel. Areas Commun. **30**(2), 280–288 (2012)

29.   C Hucher, GRB Othman, JC Belfiore, in *Proc.of IEEE International, Symposium on Information Theory (ISIT)*. AF and DF protocols based on Alamouti ST code (IEEE, Nice, 2007), pp. 1526–1530

30.   IS Gradshteuin, IM Ryzhik, *Table of integrals, series, and products (Seventh Edition)*. (Elsevier, Academic Press, New York, 2007)

31.   Z Ding, Z Yang, P Fan, HV Poor, On the performance of non-orthogonal multiple access in 5G systems with randomly deployed users. IEEE Sig. Process. Lett. **21**(12), 1501–1505 (2014)

32.   J Wu, C Yuen, B Cheng, M Wang, J Chen, Energy-minimized multipath video transport to mobile devices in heterogeneous wireless network. IEEE J. Sel. Areas Commun. **34**(5), 1160–1178 (2016)

33.   J Wu, B Cheng, C Yuen, Y Shang, J Chen, Distortion-Aware Concurrent multipath transfer for mobile video streaming in heterogeneous wireless networks. IEEE Trans. Mobile Comput. **14**(4), 688–701 (2015)

34.   J Wu, C Yuen, M Wang, J Chen, CW Chen, TCP-oriented raptor coding for high-frame-rate video transmission over wireless networks. IEEE J.Sel. Areas Commun. **34**(8), 2231–2246 (2016)

35.   S Lee, R Zhang, Cognitive wireless powered network: spectrum sharing models and throughput maximization. IEEE Trans. Cognitive Commun. and Network. **1**(3), 335–346 (2015)